The Neurotoxicity of the Venom Phospholipases A$_2$, Notexin and Taipoxin

J. B. Harris, B. D. Grubb,[1] C. A. Maltin,[2] and R. Dixon[3]

School of Neurosciences and Psychiatry, Medical School, University of Newcastle upon Tyne, Framlington Place,
Newcastle upon Tyne NE2 4HH, United Kingdom

    The presynaptically active, toxic phospholipases known as notexin and taipoxin are principal components of the venom of the Australian tiger snake and the Australian taipan respectively. The inoculation of the toxins into one hind limb of rats caused, within 1 h, the depletion of transmitter from the motor nerve terminals of the soleus muscle. This was followed by the degeneration of the motor nerve terminals and of the axonal cytoskeleton. By 24 h 70% of muscle fibers were completely denervated. Regeneration and functional reinnervation were almost fully restored by 5 days, but collateral innervation was common in the regenerated muscles, and this abnormality persisted for at least 9 months. The data provide an explanation for both the severity of neuromuscular paralysis that can accompany envenoming bites by tiger snakes and taipans and the difficulty experienced by physicians in managing the envenomed subjects. © 2000 Academic Press

Key Words: neurotoxicity; toxins; venom; phospholipases; notexin; taipoxin.

INTRODUCTION

Snake venoms are rich sources of phospholipases A$_2$ (17). Many of the phospholipases appear to have a simple digestive function (5) but some are potent presynaptically active neurotoxins with an LD$_{50}$ of 1–3 μg $\cdot$ g^{-1} (mouse iv or ip). Human victims of bites by snakes whose venoms contain large quantities of presynaptically active neurotoxins suffer a profound neuromuscular paralysis and are extremely difficult to manage. They frequently require long periods in intensive care because they do not respond well to antivenoms or to procedures that might be expected to relieve neuromus-

cular blockade such as anticholinesterases and diaminopyridine s (19, 28–30).

Acute investigations *in vivo* had suggested that the primary cause of death following the inoculation of the neurotoxic phospholipases A$_2$ was either a blockade of transmitter release or the depletion of transmitter from motor nerve terminals (4, 10, 12). In a more recent study of the neuropathological consequences of exposure to toxic phospholipases, Dixon and Harris (7) inoculated the hind limb of rats with sublethal doses of β-bungarotoxin (a neurotoxic phospholipase A$_2$ from the venom of the kraits, *Bungarus sp.*) and showed that the toxin caused the depletion of transmitter from the nerve terminals and the degeneration of nerve terminal and intramuscular axons. These observations appeared to offer an explanation for the severity of the neuromuscular paralysis and the difficulty in management of victims, but we needed to know whether this degenerative response is specific to β-bungarotoxin or is a response to the presynaptically active neurotoxins in general. We have therefore made a detailed study of the neuropathological consequences of the local inoculation of two other major neurotoxic phospholipases A$_2$, notexin (a principal neurotoxin from the venom of the Australian tiger snake) and taipoxin (the principal neurotoxin from the venom of the taipan). These toxins are also myotoxic (6, 11) and the study of myotoxicity has overshadowed the neurotoxic potential of the toxins. We have shown that nerve terminal and axonal degeneration is a prominent feature of the toxicology of this class of natural toxins. We have been able to document the time scale of degeneration and have shown that degeneration is very rapid in onset and is widespread in muscles exposed to the toxins.

MATERIALS AND METHODS

Animals

Female Wistar rats (90–100 g) were obtained from an accredited breeder and maintained in accordance with the requirements of the Animals (Scientific Procedures) Act of 1986. A total of 65 animals were used in this study. Muscles from 30 of them were used for electron

---

[1] Present address: Department of Cell Physiology and Pharmacology, University of Leicester, Leicester LE1 9HN.
[2] Present address: Rowett Research Institute, Bucksburn, Aberdeen AB21 9SB.
[3] Present address: Wyeth-Ayerst Research, Huntercombe Lane South, Taplow, Berkshire SL6 0PH.

microscopy, muscles from 19 were used for the study of the innervation of the muscle fibers, and muscles from 16 were used for routine histology and for electrophysiology. Animals had free access to food and water and were under the day-to-day supervision of a veterinarian.

Nerve-Muscle Preparation in Vivo

The soleus muscle was used to study the responses of skeletal muscle and its innervation following the inoculation of either notexin or taipoxin. The toxins (2 µg in 0.2 ml of 10 µg ml^{-1} in 0.9% w/v NaCl) were inoculated subcutaneously into the dorsolateral aspect of one hind limb so as to bathe the underlying soleus muscle in toxin (11). The contralateral soleus muscle acted as the control. At various times after inoculation (0.5 h–21 days) the ipsi- and contralateral muscles were removed, pinned onto dental wax at 1.2× resting length, and prepared for either transmission electron microscopy or the demonstration of acetylcholinesterase (AChE), acetylcholine receptor (AChR), or axonal neurofilament.

Transmission Electron Microscopy

Tissues for electron microscopy were fixed in Karnovsky's fluid (16) for 1 h. End-plate AChE was identified using the technique of Strum and Hall-Craggs (27). Regions of the muscles containing the brick-red deposits identifying end plates were cut out of the muscles in small blocks (dimensions 1 × 1 × 2 mm) and fixed for a further 30 min. The blocks were transferred to OsO_4 for secondary fixation, dehydrated in graded alcohol, and embedded in araldyte resin. The blocks were trimmed until the regions containing end plates were reached and ultrathin sections (50–70 nm) were prepared of stained regions for examination in a JEOL 1200 Ex transmission electron microscope.

Combined AChR and Neurofilament Staining

Isolated muscles were pinned at 1.2× resting length onto dental wax and fixed in paraformaldehyde (0.5% w/v in 0.1 M phosphate-buffered saline (PBS)) for 10 min. The muscles were then teased into 3–4 bundles of muscle fibers and returned to fixative for a further 20 min. The muscle fiber bundles were rinsed in 0.1 M PBS and further teased into smaller bundles of 10–12 fibers. These were permeabilized in absolute ethanol for 10 min at −18°C and again rinsed in PBS before being transferred to an incubation medium (3% w/v bovine serum albumin and 0.1 M lysine in PBS) containing mouse anti-neurofilament antibody (volume ratio 100:1) and incubated overnight at 4°C. The following

morning the muscle fiber bundles were rinsed in PBS and incubated for 1 h at 20°C in FITC-α bungarotoxin (to label AChR) and rhodamine-labeled rabbit anti-mouse polyclonal IgG (to label the anti-neurofilament antibodies). The bundles were washed again in PBS, mounted in Vectashield onto glass slides, and examined under a Bio-Rad MRC 600 confocal scanning laser microscope.

Combined AChE and Silver Staining

In some regenerating muscles, the technique of Pestronk and Drachman (20) was used to identify the end-plate region and the relevant motor axons. In brief, 10-µm-thick frozen sections were mounted onto slides coated with EDTA. The mounted sections were incubated in Na_2SO_4 (20% w/v in distilled H_2O), rinsed in deionized water, and then incubated in Pestronk and Drachman's AChE medium (20). The sections were then dehydrated in graded alcohols before being impregnated with silver (20). In this technique AChE is visualized as a translucent blue deposit and axons are black.

Combined AChR and AChE Staining

Frozen sections (10 µm) of soleus muscles were mounted onto glass slides. The sections were incubated (1 h room temperature) with polyclonal rabbit anti-rat AChE antibodies diluted 1:500 in PBS containing 3% BSA and 0.1 M lysine. The sections were rinsed with PBS and incubated for 1 h at room temperature with 1:100 swine anti-rabbit antibody and FITC-α bungarotoxin. The sections were washed with PBS, fixed for 15 min in 1% paraformaldehyde, mounted in Vectashield, and examined under a standard fluorescence microscope.

Electrophysiology

Electrophysiological techniques were used to search for evidence of multiple innervation before and at various times after the inoculation of notexin or taipoxin. Isolated soleus muscles were mounted in a constant flow bath perfused with a bathing solution of composition (mM) K$^+$ 5.0; Na$^+$ 150; Ca^{2+} 2.0; Mg^{2+} 1.0; Cl$^-$ 148; $H_2PO_4^-$ 1.0; HCO_3^- 12; glucose 11. Solutions were equilibrated by bubbling with 5% CO_2 in O_2 and were maintained at room temperature.

Glass microelectrodes (resistance ca. 10 M Ω) were inserted into the end-plate regions of cut fiber preparations (1). The distal stump of the motor nerve was stimulated via a suction electrode and the evoked end-plate potentials were recorded. Evidence for the presence of multiple innervation was sought by slowly increasing the strength of the stimulating pulse from
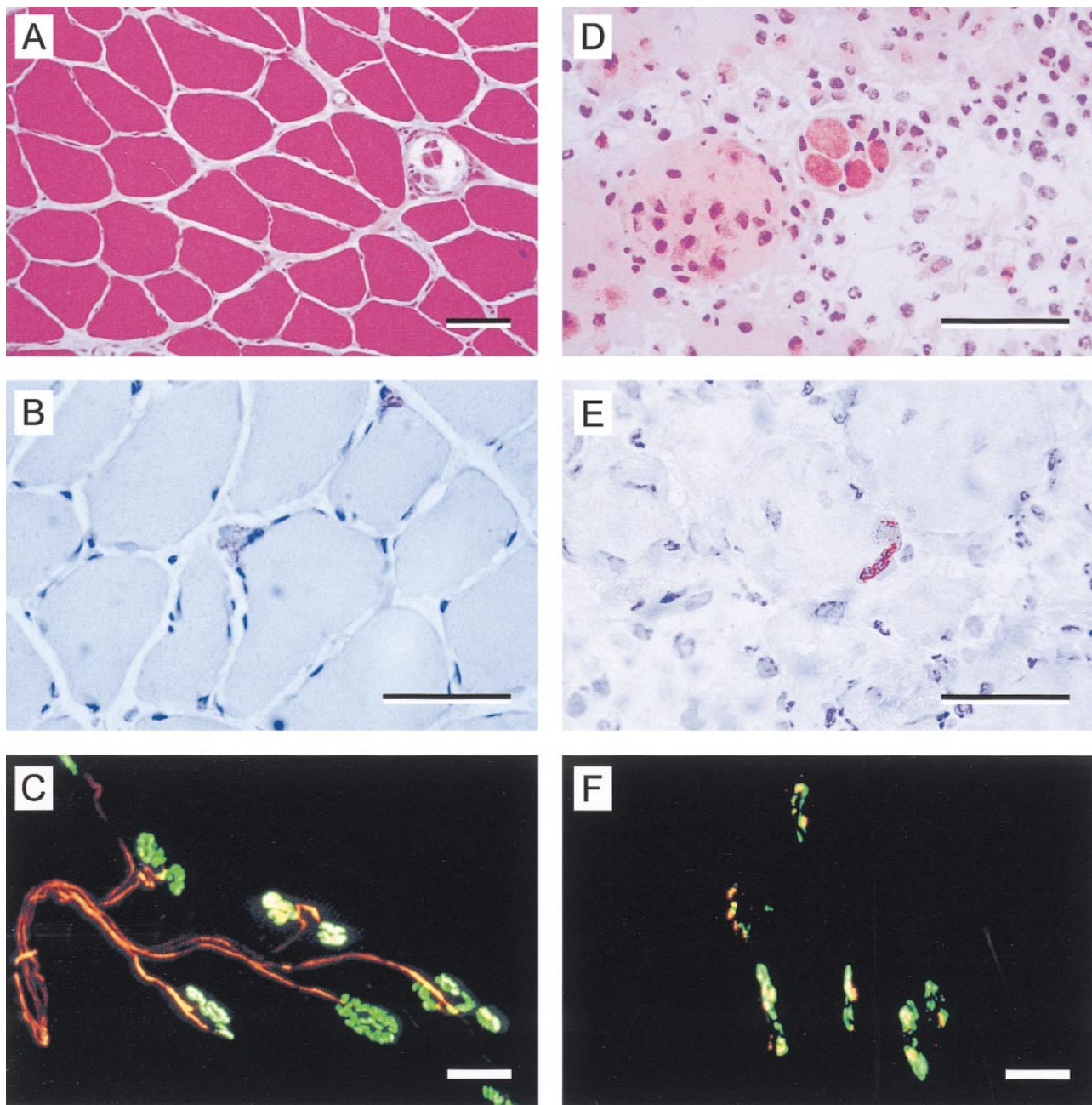
FIG. 1. Transverse sections of contralateral soleus muscles (A, B) and toxin treated muscles (D, E) 24 h after a single inoculation of notexin (2.0 μg sc) into the anterolateral aspect of one lower hind limb. A is a transverse section of a frozen control muscle stained with H&E. Note the regular staining and the slightly angular muscle fibers. D is a frozen section of the opposite soleus muscle inoculated with notexin as described above. Note the degenerating extrafusal muscle fibers filled with phagocytic cells. B and E are transverse frozen sections stained to show AChE activity as a brick-red deposit. ACE is localized to the junctional basal lamina. Note its persistence in the degenerated muscle fibers at 24 h. C and F are of teased bundles of lightly fixed muscle fibers in which AChR are labeled with FITC–α-BTX and neurofilament protein is labelled with anti-neurofilament Ab and a 20-rhodamine-labelled Ab. Note the loss of labelling in F. Scale bars, 50 μm in all micrographs.

subthreshold levels and seeking evidence of more than one all-or-nothing end-plate potential (21).

Toxins, Antibodies, and Other Reagents

Notexin and taipoxin were a gift. The toxins were isolated from the venoms of the Australian tiger snake, *Notechis scutatus scutatus,* and the Australian taipan, *Oxyuranus scutellatus scutellatus,* respectively, by Dr. D. Eaker, Uppsala, Sweden. Murine monoclonal anti-neurofilament antibody was a gift from Prof. Leigh (Institute of Psychiatry, London). It recognizes both phosphorylated and nonphosphorylated forms of heavy
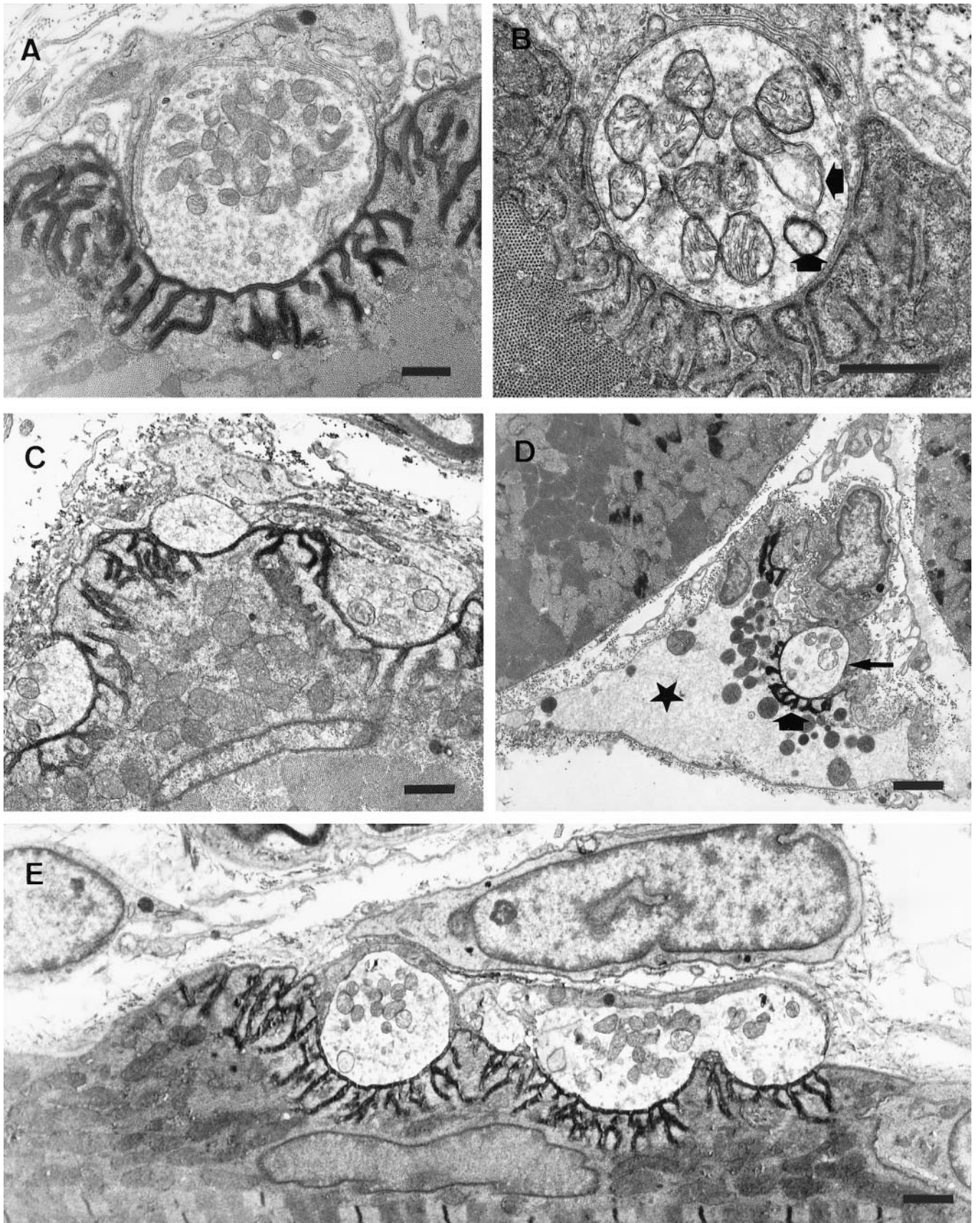
FIG. 2. Electron micrographs of neuromuscular junctions in rat soleus muscle fibers 1 h after the inoculation of notexin or taipoxin (2.0 μg sc) into the anterolateral aspect of one hind limb. A (control) shows the normal organization of the nerve terminal. Note the depletion of synaptic vesicles from terminals in toxin-treated muscles (B,C) and the normal appearance of the muscle fibers in most sections. B illustrates

neurofilament. It is commercially available as RT97 from Boehringer Mannheim, Germany. The polyclonal rabbit antibody used to recognize junctional AChE was a gift from Dr J. Massoulie, Ecole Normale Supérieure, Paris. Fluorescein isothiocyanate-conjugated α-bungarotoxin (FITC–α-BTX) was from Molecular Probes (Eugene, OR). Swine anti-rabbit polyclonal antibody conjugated with rhodamine and rabbit anti-mouse polyclonal antibody conjugated with rhodamine were from Dako (Buckinghamshire, UK). Vectashield aqueous mountant was from Vector Laboratories (Burlingame, CA). Other reagents were from regular commercial suppliers and were routinely of the highest grade available.

Specificity of Major Reagents

The specificity of FITC–α-BTX was checked by labeling frozen sections of soleus muscles with a polyclonal rabbit antibody to rat brain AChE and TRITC–swine anti-rabbit IgG. This enabled end plates to be unequivocally and specifically labeled. The sections were then incubated for 60 min in PBS with or without native α-BTX (30 μg ml^{-1}) or β-BTX (30 μg ml^{-1}). The sections were rinsed and incubated for 30 min with FITC–α-BTX. Control sections and sections incubated with native β-BTX were labeled with FITC–α-BTX at every AChE-identified end plate. Sections incubated with native α-BTX did not label with FITC–α-BTX. The specificity of the anti-neurofilament antibody was originally demonstrated by Western blotting. The antibody recognizes both phosphorylated and nonphosphorylated forms of 160- and 200-kDa neurofilaments. It does not recognize tubulin.

The secondary antibodies were preabsorbed with normal rat serum before use. There was no labeling with the secondary antibodies in any preparation that had not been previously exposed to the relevant primary antibody.

Collection and Analysis of Data

To ensure that morphological data obtained during this study were truly representative, at least three muscles were used at each time point. For electron microscopy, blocks of tissue were randomly selected from each muscle and screened for the presence of end plates. Those blocks containing end plates (identified by the presence of positive staining for AChE) were used to prepare thin sections of tissue for electron microscopy. The tissue blocks were selected and sections were examined blind. Between 10 and 40 randomly encountered end plates were photographed from

each muscle. The photomicrographs were examined blind and end plates were classified as "normal" if the terminals were filled with synaptic vesicles and undamaged mitochondria and "damaged" if the terminals were devoid of vesicles, contained damaged mitochondria, or were filled with degenerating subcellular organelles. Data on AChR and neurofilament distribution were similarly collected from muscle fiber bundles teased from at least 3 muscles. A typical muscle yielded approximately 20–30 useable bundles of 10–12 muscle fibers. Images were selected for analysis and photography only if the end plate, identified from FITC–α-BTX labeling, was *en face.* These data were collected blind and analyzed later by examination of stored images.

It should be acknowledged that the pathology we were recording was so significant that the term "blind" cannot be considered absolute.

RESULTS

There were no recognizable differences in the response of muscle fibers, nerve terminals, or intramuscular axons to exposure, respectively, to notexin or taipoxin. The results are, therefore, not differentiated.

Normal Tissue

Transverse sections of control soleus muscles revealed the regular slightly angular profile of the individual muscle fibers (Fig. 1A) and the presence of acetylcholinesterase where the section contained neuromuscular junctions (Fig. 1B). Teased bundles of muscle fibers processed for the immunocytochemical demonstration of neurofilament and the colabeling of acetylcholine receptors, confirmed the normal pattern of innervation—one axon per muscle fiber (Fig. 1C).

The Toxin-Induced Degeneration of Muscle and Nerve

The myotoxic activities of notexin and taipoxin have been described at length (11, 13, 14), and will be described only briefly here. Degeneration of muscle fibers began 1–3 h after inoculation. By 6 h, most muscle fibers in the muscles were damaged and, by 12–24 h, almost every muscle fiber in the muscles was destroyed (Fig. 1D). Longitudinal sections of muscles cut 12–24 h after inoculation of toxin revealed areas of hypercontracted contractile material invaded by phagocytic cells of various kinds interspersed with regions of empty basal lamina tube, caused by the tearing of myofibrils by adjacent areas of hypercontraction (11, 14).

---

clearly the loss of cristae in the damaged mitochondria (heavy arrows). D represents a muscle fiber in which the internal organization of the fiber is disrupted (star). The damaged nerve terminal (arrow) sits in a "normal" junction (heavy arrow). The fiber consists of a collapsed basal lamina tube. AChE staining was used in most preparations to aid in the identification of the junctions, which were marked by a black deposit in the junctional folds. Scale bars, 1 μm in all micrographs.

AChE, a component of the junctional basal lamina, was readily identified in both transverse and longitudinal sections of muscle at all stages of degeneration and regeneration (Fig. 1E), presumably reflecting the survival of the basal lamina of the degenerating muscle fibers. Slater and Allen (25) reported that AChR and the junctional plasma membrane often survived exposure to the toxic phospholipase notexin. This was confirmed in this study. Thus, at 24 h, when muscle fibers were totally destroyed, reactivity to AChR persisted at 44/47 identifiable neuromuscular junctions encountered in tissue sections. Although, AChR could be routinely identified in bundles of teased muscle fibers the intramuscular axons could not be labeled with anti-neurofilament antibodies (Fig. 1F).

To determine whether the intramuscular axons had been destroyed by the toxins, axonal integrity was studied using silver staining. Six normal (contralateral) muscles were sectioned for light microscopy, and 314 junctional regions were identified by AChE staining. Silver staining was used to identify motor axons. Eighty-eight percent of the junctional regions were clearly innervated. In contrast of a total of 51 junctions examined in 3 muscles 24 h after the inoculation of toxin, only 6% were clearly innervated; in the remainder, no intact axons could be identified.

To study the early stages of the response of the nerve terminals to exposure to the toxins, animals were killed at intervals after the inoculation of either taipoxin or notexin and electron micrographs of more than 300 randomly chosen motor nerve terminals were prepared. At 1 h 100 nerve terminals were studied. Sixteen of the terminals were physically damaged, exhibiting morphologically abnormal mitochondria and/or lysosomal structures. Motor nerve terminals were completely absent from three otherwise normal junctions. Fifty-eight of the terminals were devoid of synaptic vesicles except for the presence of clathrin-coated "Ω" profiles and occasional internal clathrin-coated vesicles but were otherwise indistinguishable from normal. The remaining nerve terminals were without obvious pathology. At this stage, despite the damage to nerve terminals, there was no morphological evidence of damage to most underlying muscle fibers (Fig. 2).

By 3–6 h after the inoculation of the toxins, 36% of the motor nerve terminals examined (total $n = 100$) were physically damaged. Some terminals were completely devoid of internal architecture, some were filled with damaged mitochondria and mitochondrial debris, and some contained large lysosomal-like bodies. Many junctional clefts were invaded by Schwann cell processes. It was of significance that severely damaged nerve terminals could be seen on either apparently undamaged muscle fibers or necrotic ones. By 24 h nearly 70% of nerve terminals were destroyed, exhibiting all the features described above, and the muscle fibers were also damaged (Fig. 3). Electron microscopy also showed that the junctional region of the muscle fiber was remarkably resistant to the toxins. Despite the loss of extrajunctional plasma membrane and internal architecture, junctional folds were often intact and segments of plasma membrane remained. In such cases, phagocytic cells apparently clearing debris from between adjacent junctional folds were often seen (Fig. 3D).

The Regeneration of Muscle and Its Innervation

Regeneration of the skeletal muscle began 2–3 days after inoculation with the formation of multinucleate myotubes within the surviving basal lamina tubes. The muscle fibers were centrally nucleated (Fig. 4A) and the site of the "old" end plate could be identified by the persistence of AChE activity in the surviving basal lamina (Fig. 4B).

By 5 days combined AChE/Ag staining (20) showed that 59 of 67 (i.e., 88%) junctions examined were reinnervated, a level of reinnervation consistent with physiological data acquired by Grubb *et al.* (9). At this stage pre- and ultraterminal sprouting of the regenerating axons was seen at more than 30% of all junctions. Sprouts were often very long (>200 μm) and usually orientated along the appropriate muscle fiber (Fig. 4C). The degree of sprouting fell to 5% at 10 days and was not seen at all by 14 days.

By 21–28 days, the process of regeneration was complete. Muscle fibers were identical to control muscle fibers with the exception of the presence of centrally located muscle nuclei (Fig. 4D). AChE was located specifically to the junctional region of the muscle fibers (Fig. 4E). Innervation, however, was abnormal. Collateral innervation (the innervation of a number of adjacent muscle fibers by a single axon), first seen at around 7 days after the inoculation of toxin, was commonly seen at 21 days (Fig. 4F) and persisted for at least 9 months. Multiple innervation (the innervation of a single muscle fiber by more than one axon) was, however, very rare. Morphological studies of more than 500 junctions between 5 and 21 days after the inoculation of toxin identified only 8 unequivocal examples of multiple innervation. Physiological studies of end-plate potentials similarly identified only 7 examples of multiple innervation of 115 junctions studied over the period 5–10 days post toxin injection (Fig. 5). No examples of multiple innervation were seen using either morphological or physiological criteria prior to 5 days or after 10 days.

DISCUSSION

The objective of this study was to determine the morphological correlates of neurotoxic activity of the
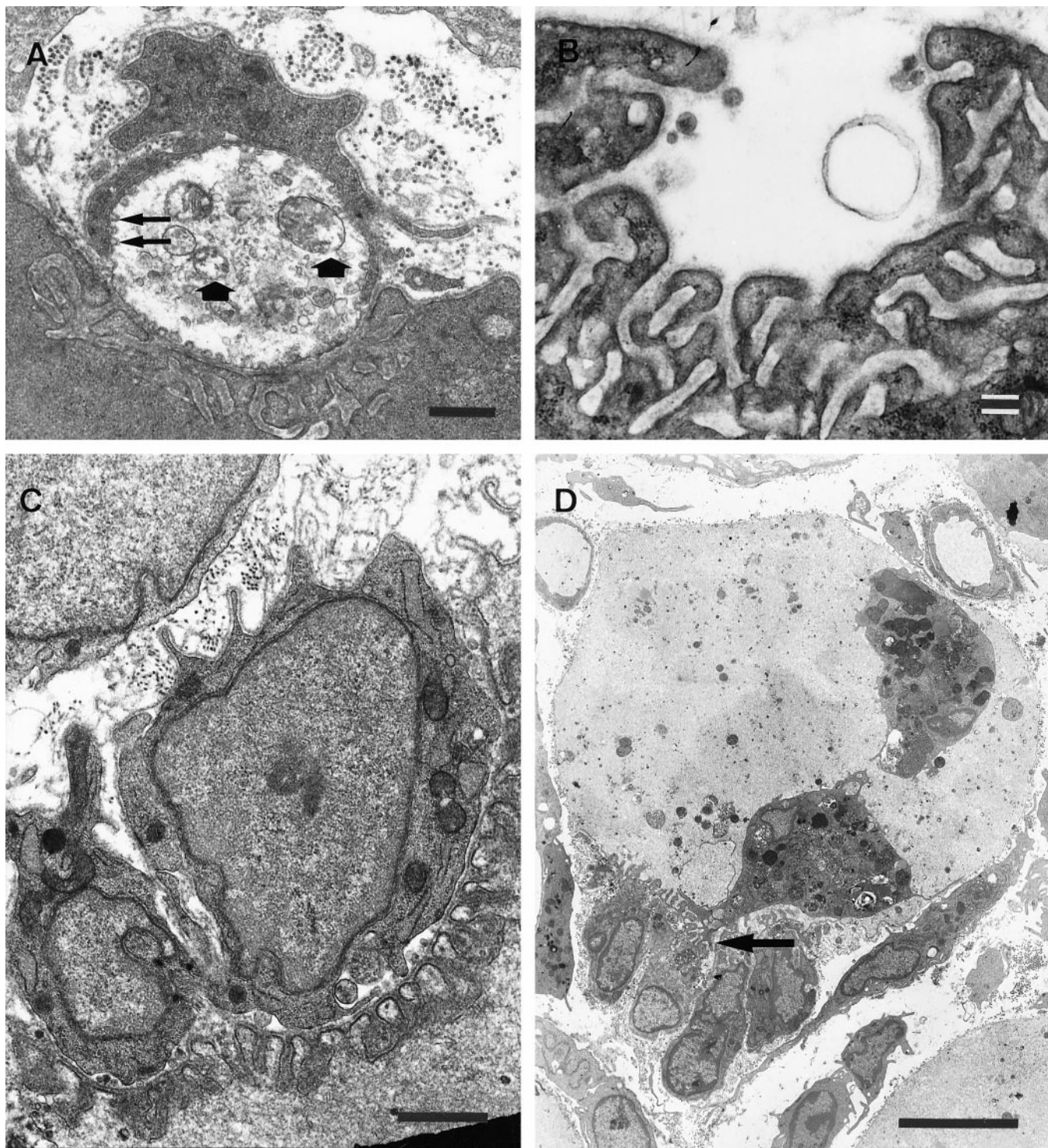
FIG. 3. Electron micrographs of neuromuscular junctions in rat soleus muscle fibers 24 h after the inoculation of notexin or taipoxin (2.0 μg, sc) into the anterolateral aspect of one hind limb. A illustrates a nerve terminal containing few free synaptic vesicles and degenerating mitochondria (heavy arrows). There are numerous coated "Ω" profiles on the nerve terminal membrane (fine arrows). The muscle fiber is hypercontracted. B shows a junction devoid of nerve terminal. C and D illustrate the preservation of junctional organization even after gross degenerative change to the muscle fiber. In each case, primary clefts are occupied by highly active Schwann cells. D shows a fiber filled with phagocytic cells, one of which has finger-like projections entering the junctional folds (arrow). The plasma membrane of this muscle fiber is intact in the synaptic region but has gone from the presynaptic region. Scale bars, 2 μm in all micrographs.
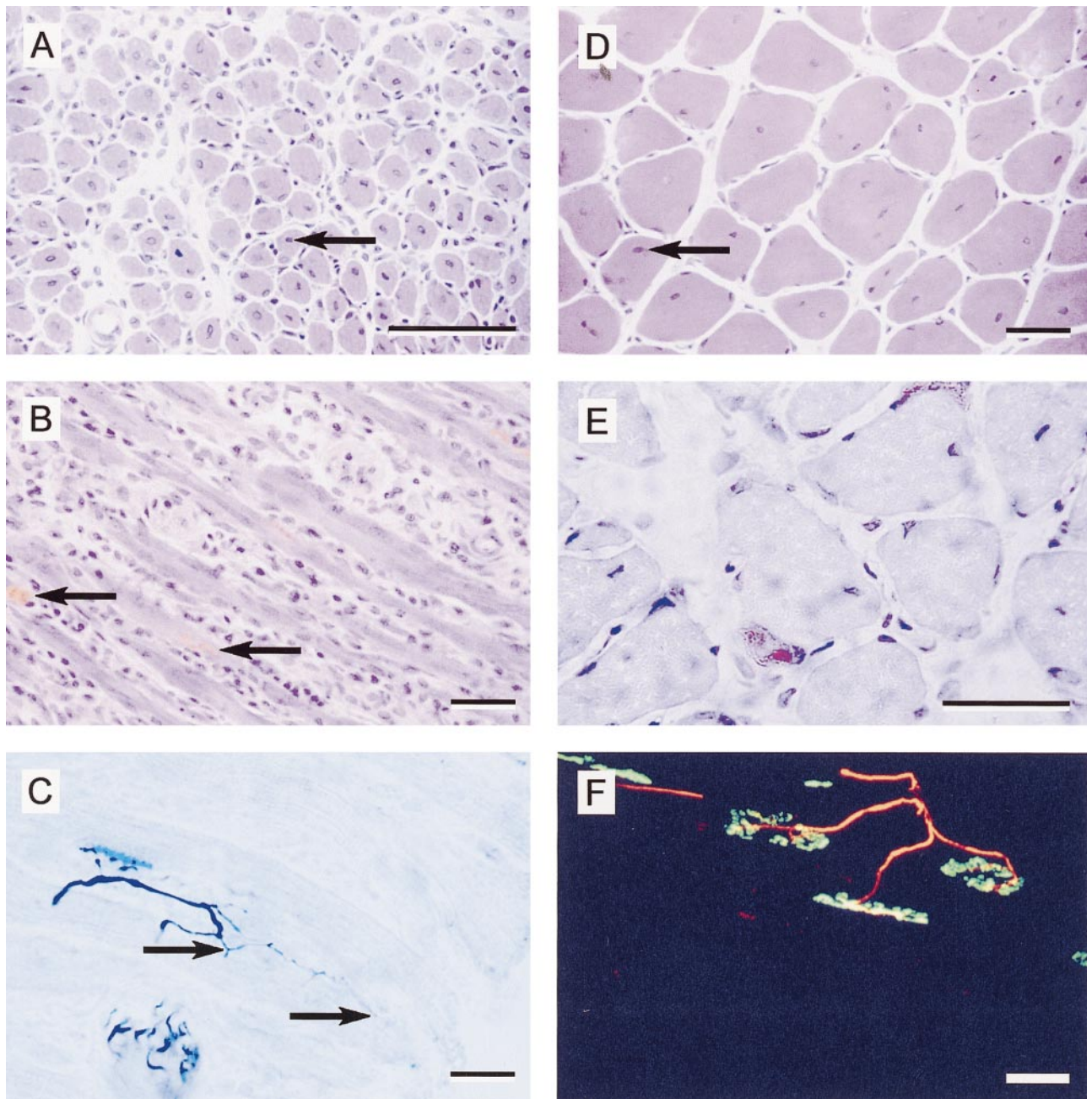
FIG. 4. Muscle sections (A–E) and bundles of muscle fibers (F) prepared from soleus muscles (3–5 days) (left-hand column and 21 days (right-hand column)) after a single inoculation of notexin (2.0 µg sc) into the anterolateral aspect of one lower hind limb. A and D were stained with H&E and illustrate the rapid growth of the muscle fibers and the persistent central nucleation (arrows). B and E (respectively, longitudinal and transverse) have been stained to show AChE activity. Even at 3 days (B) AChE activity is retained (arrows). C has been stained with silver to illustrate the extensive sprouting seen at early stages of reinnervation. The axon enters from the left and immediately innervates one fiber at the junction (identified by the blue-stained AChE). A thick axonal branch continues to innervate an adjacent fiber from which a long slender axonal process emerges (arrows). F is a teased bundle of fibers in which AChR are labeled with FITC-α–bungarotoxin (green) and in which axonal neurofilament is labeled with rhodamine-conjugated anti-neurofilament antibody (red). The axon emerging from the top of the figure divides into three major branches that innervated a group of adjacent muscle fibers. Scale bars, 50 µm in A, D, and E; 25 µm in B, C, and F.

toxic phospholipases A_2 notexin and taipoxin and to establish the time course of any degenerative changes.

We have shown that within 1 h of inoculation of the toxins *in vivo,* many nerve terminals already exhibited signs of physical damage, and the majority of the surviving terminals were devoid of synaptic vesicles. Clathrin-coated Ω pits were common in the "empty" nerve terminals and a few large, clathrin-coated vesicles could be identified within the nerve terminal. We have also shown that by 24 h large numbers of nerve
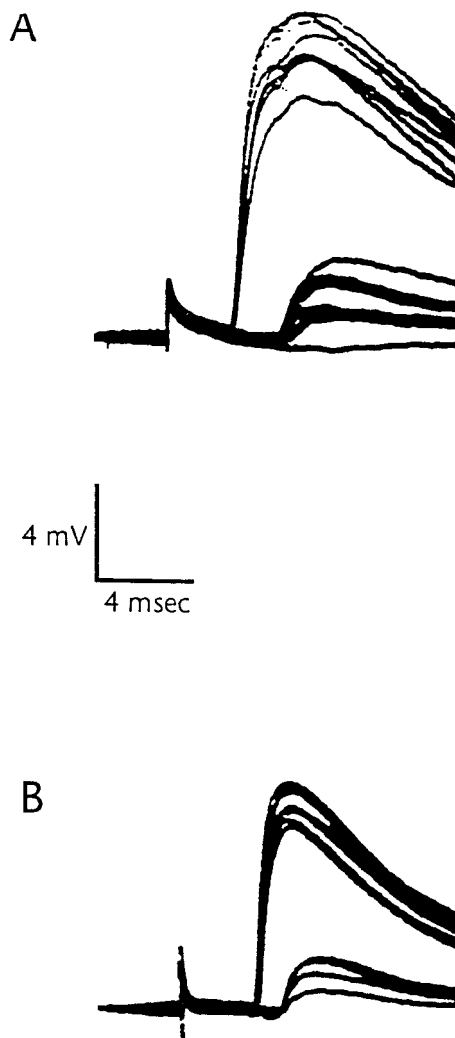
A

4 mV

4 msec

B

FIG. 5. End-plate potentials recorded from different rat soleus muscle fibers 5 (A) and 7 days (B) after the inoculation of notexin (2.0 μg, sc) into the anterolateral aspect of one hind limb. In each case two populations of end-plate potentials, distinguishable by size and latency, could be recruited by varying the intensity of stimulation.

terminals and intramuscular axons were totally destroyed, leaving ca. 70% of muscle fibers devoid of even the remnants of motor innervation. The preservation of the postjunctional component of the neuromuscular junction, even in very damaged muscle fibers, confirms some early observations by Slater and Allen (25). We still have no explanation for the observation.

The early loss of synaptic vesicles can have several origins: excessive rates of exocytosis; failure of recycling of fused vesicles after the discharge of their contents; and destruction of vesicles within the nerve terminals are the most obvious possibilities. The loss is unlikely to be the result of only an excessive rate of exocytosis. The increase in mepp frequency caused by the neurotoxic phospholipases A_2, β-bungarotoxin, for example, rarely exceeds 3× normal and the quantal content, "m," of end-plate potentials is typically only

doubled (2). It is difficult to believe that such modest increases in mepp frequency and mepp quantal contents would lead to the depletion of synaptic vesicles from the motor nerve terminal. The presence of large numbers of clathrin coated Ω profiles on the nerve terminal plasma membrane and the presence of large clathrin-coated vesicles in the nerve terminal suggest that the recycling of synaptic vesicles is impaired; the combination of enhanced release and impaired recycling might be sufficient to empty the nerve terminal.

Is it possible that synaptic vesicles are destroyed *in situ* in the nerve terminal? There are two possible mechanisms by which the vesicles are destroyed: one is the internalization of the toxins and the other is the activation of pathogenic second messenger systems. The possibility that the toxins are internalized and then released into the cytosol to gain access to the membranes of subcellular organelles such as mitochondria and synaptic vesicles is very attractive (26) but there is considerable indirect evidence that the toxic phospholipases are not internalised (8, 15, 22, 24).

The possibility that exposure to the toxins leads to the activation of a number of pathogenic secondary messenger systems is much more attractive. The toxins all show pronounced phospholipase A_2 activity and have been shown to be capable of hydrolyzing both phospholipid micelles and intact biological membrane systems (13). Notexin binds selectively to the plasma membranes of skeletal muscle fibers (6) and it seems reasonable to presume that the neurotoxic phospholipases bind to the plasma membrane of the nerve terminal and thereby gain access to the membrane phospholipids. Hydrolytic activity, resulting in the formation of lysophosphatides and the release of free fatty acids, would be expected to cause an early reduction in membrane anisotropy, a loss of ion gradients, the influx of Na^+ and Ca^{2+}, depolarization, and the activation of a large number of secondary processes such as Ca^{2+}-activated proteolytic activity (3, 18, 23).

A cascade of events as outlined above would also explain the degeneration of the nerve terminal. The uncontrolled entry of Ca^{2+} would not only enhance transmitter release but would lead to mitochondrial damage (31). The activation of proteolysis via Ca^{2+}-activated proteases, together with elevated phosphorylation caused by lysophosphatide-induced synthesis of cyclic AMP, would initiate the proteolytic degradation of neurofilament proteins.

The regeneration of the terminal axons was rapid and apparently efficient, but the collateral sprouting seen in the fully regenerated muscles was unexpected. It is not clear at present whether the sprouting reflects the enlargement of some motor units at the expense of others or the concentration of motor units into a smaller area of muscle. This question is currently under investigation.

Our data show that degeneration of the motor nerve

terminal and intramuscular axon is an extremely common response to exposure to the toxic phospholipases, and it explains why envenoming bites by snakes whose venoms are rich in such toxins cause such severe and prolonged neuromuscular paralysis and why the patients are so difficult to treat (19, 28–30). Slowing the rate of degenerative change and increasing the rate of reinnervation should be important strategic aims for improving the clinical management of such patients.

In the longer term, it is important to learn whether the regenerated, reorganized motor units are larger than normal, because excessively large motor units are inherently unstable. If this instability leads to the early demise of the motoneuron, the long-term consequences for the victim are significant.

ACKNOWLEDGMENTS

REFERENCES

1. Barstad, J. A. B. 1962. Presynaptic effect on the neuromuscular transmitter. *Experientia* **18:** 579–580.

2. Chang, C. C., T. F. Chen, and C. Y. Lee. 1973. Studies of the presynaptic effect of β-bungarotoxin on neuromuscular transmission. *J. Pharm. Exp. Ther.* **184:** 339–345.

3. Corr, P. B., R. B. Gross, and B. E. Sobel. 1984. Amphipathic metabolites and membrane dysfunction in ischemic myocardium. *Circ. Res.* **55:** 135–154.

4. Cull-Candy, S. G., J. Fohlman, D. Gustavsson, R. Lüllman-Rauch, and S. Thesleff. 1976. The effects of taipoxin and notexin on the function and fine structure of the murine neuromuscular junction. *Neuroscience* **1:** 175–180.

5. Davidson, F. F., and E. A. Dennis. 1991. Structure, function and mode of action of snake venom and other phospholipases A₂. In *Handbook of Natural Toxins, Vol. 5. Reptile Venoms and Toxins* (A. T. Tu, Ed.), pp. 107–145. Dekker, New York.

6. Dixon, R., and J. B. Harris. 1996. Myotoxic activity of the toxic phospholipase, notexin, from the venom of the Australian tiger snake. *J. Neuropathol. Exp. Neurol.* **55:** 1230–1237.

7. Dixon, R., and J. B. Harris. 1999. Neurotoxic activity of the toxic phospholipase A₂, β-bungarotoxin: Its clinical significance. *Am. J. Pathol.* **154:** 447–455.

8. Esquerdera, J. E., C. Solsana, and J. Marsal. 1982. Binding of β-bungarotoxin to *Torpedo* electric organ synaptosomes. A high resolution autoradiographic study. *Neuroscience* **7:** 751–758.

9. Grubb, B. D., J. B. Harris, and I. S. Schofield. 1991. Neuromuscular transmission at newly formed neuromuscular junctions in the regenerating soleus muscle of the rat. *J. Physiol.* **441:** 405–421.

10. Hamilton, R. C., A. J. Broad, and S. K. Sutherland. 1980. Effects of Australian eastern brown snake (*Pseudonaja textilis*) venom on the ultrastructure of nerve terminals on the rat diaphragm. *Neurosci. Lett.* **19:** 45–50.

11. Harris, J. B., and M. A. Johnson. 1978. Further observations on the pathological responses of rat skeletal muscle to toxins isolated from the venom of the Australian tiger snake, *Notechis scutatus scutatus*. *Clin. Exp. Pharm. Phys.* **5:** 587–600.

12. Harris, J. B., E. Karlsson, and S. Thesleff. 1973. Effects of an isolated toxin from Australian tiger snake (*Notechis scutatus scutatus*) venom at the mammalian neuromuscular junction. *Br. J. Pharmacol.* **47:** 141–146.

13. Harris, J. B., and C. A. MacDonell. 1981. Phospholiphase A₂ activity of notexin and its role in muscle damage. *Toxicon* **19:** 419–430.

14. Harris, J. B., and C. A. Maltin. 1982. Myotoxic activity of the crude venom and the principal neurotoxin, taipoxin, of the Australian taipan, *Oxyuranus scutellatus*. *Br. J. Pharmacol.* **76:** 61–75.

15. Howard, B. D., and W. C. S. Wu. 1976. Evidence that β-bungarotoxin acts at the exterior of nerve terminals. *Brain Res.* **103:** 190–192.

16. Karnovsky, M. J. 1965. A formaldehyde-glutaraldehyde fixative of high osmolarity for use in electron microscopy. *J. Cell Biol.* **27:** 137a.

17. Mebs, D., and I. Claus. 1991. Amino acid sequences and toxicities of snake venom components. In *Snake Toxins* (A. L. Harvey, Ed.), pp. 425–447. Pergamon Press, New York.

18. Ordway, R. W., J. J. Singer, and J. V. Walsh, Jr. 1991. Direct regulation of ion channels by fatty acids. *TINS* **14:** 96–100.

19. Pearn, J. 1971. Survival after snake bite with prolonged neurotoxic envenomation. *Med. J. Aust.* **2:** 259–261.

20. Pestronk, A., and D. B. Drachman. 1978. Motor nerve sprouting and acetylcholine receptors. *Science* **199:** 1223–1225.

21. Redfern, P. A. 1970. Neuromuscular transmission in new-born rats. *J. Physiol. (Lond.)* **209:** 701–709.

22. Rugulo, M., J. O. Dolly, and D. G. Nicholls. 1986. The mechanism of action of β-bungarotoxin at the presynaptic plasma membrane. *Biochem. J.* **233:** 519–523.

23. Sedlis, S. P., P. B. Corr, B. E. Sobel, and G. G. Ahmuda. 1983. Lysophosphatidyl choline potentiates Ca²⁺ accumulation in rat cardiac myocytes. *Am. J. Physiol. (Heart Circ. Physiol.)* **13:** H32–38.

24. Simpson, L. L., G. T. Lautenslager, I. I. Kaiser, and J. L. Middlebrook. 1993. Identification of the site at which the phospholipase A₂ neurotoxins act to produce their neuromuscular blocking effects. *Toxicon* **31:** 13–26.

25. Slater, C. R., and E. Allen. 1985. Acetylcholine receptor distribution on regenerating mammalian muscle fibers at sites of mature and developing nerve–muscle junctions. *J. Physiol. (Paris)* **80:** 238–246.

26. Strong, P. N., and R. B. Kelly. 1977. Membranes undergoing phase transitions are preferentially hydrolyzed by beta-bungarotoxin. *Biochim. Biophys. Acta.* **469:** 231–235.

27. Strum, J. M., and E. C. B. Hall-Craggs. 1982. A method of demonstrating motor endplates for light and electron microscopy. *J. Neurosci. Methods* **6:** 305–309.

28. Trevett, A. J., D. G. Lalloo, N. C. Nwokolo, S. Naragi, I. H. Kevau, R. D. G. Theakston, and D. A. Warrell. 1995. The efficacy of anti-venom in the treatment of bites by the Papuan taipan (*Oxyuranus scutellatus canni*). *Trans. R. Soc. Trop. Med. Hyg.* **89:** 322–325.

29. Trevett, A. J., D. G. Lalloo, N. C. Nwokolo, S. Naragi, I. H. Kevau, R. D. G. Theakston, and D. A. Warrell. 1995. Electrophysiological findings in patients envenomed following the bite of a Papuan taipan (*Oxyuranus scutellatus canni*). *Trans. R. Soc. Trop. Med. Hyg.* **89:** 415–417.

30. Trevett, A. J., D. G. Lalloo, N. C. Nwokolo, S. Naragi, I. H. Kevan, R. D. G. Theakston, and D. A. Warrell. 1995. Failure of 3,4-diaminopyridine and edrophonium to produce significant clinical benefit in neurotoxicity following the bite of Papuan taipan (*Oxyuranus scutellatus canni*). *Trans. R. Soc. Trop. Med. Hyg.* **89:** 444–446.

31. Wrogemann, K., and S. D. J. Penna. 1976. Mitochondrial calcium overload: A general mechanism for cell necrosis in muscle disease. *Lancet* **1:** 672–674.